XLIII CILAMCE
21-25, November, 2022
FOZ DO IGUAÇU - PR - BRAZIL

A Timoshenko Beam Formulation with 3D Response for Linear and Nonlinear Materials

Mauro Schulz[1]

[1]*Dept. of Civil Engineering, Fluminense Federal University*
Rua Passo da Pátria, 156 - Bloco D, 24210-240, Niterói/RJ, Brazil
mschulz@id.uff.br

Abstract. Beam finite elements are computationally efficient, widely used, and sufficiently accurate for many applications. The intrinsic a-priori assumptions and simplifications of classical beam theories do not always represent the actual three-dimensional stress-strain distributions. The cross-section of the Euler-Bernoulli beam remains both plane and orthogonal to the beam axis. This theory does not account for shear deformation, which is considered by Saint-Venant's solution. Timoshenko beam theory includes the rotation of the cross-section, which remains plane. This assumption yields an average shear strain, which does not correspond with the actual three-dimensional distribution of shear strains. Shear coefficients can be adopted as a correction for beams made of linear materials. However, the analysis of beams of nonlinear materials must consider the three-dimensional stress-strain relationships at each point. An integrated formulation of a beam element with three-dimensional response is discussed. The arbitrary cross-section of the corresponding Timoshenko beam element remains neither plane nor orthogonal to the beam axis. The element kinematics is defined by two fields: the displacement shapes of the cross-sections and the axial functions of their corresponding averaged movements. The deformed displacement shapes are obtained by minimizing the potential energy of a beam slice submitted to the compatibility constraints of the kinematics framework. Higher order models reproduce the three-dimensional distribution of stresses and strains of Saint-Venant's solution for concentrated loads and Michell's solution for uniformly loaded beams. The solution also agrees with three-dimensional finite element models with idealized boundary conditions. This paper presents improvements that simplify the theory, focuses on first-order linear and nonlinear analyses, and discusses some examples.

Keywords: Timoshenko beam, three-dimensional response, nonlinear analysis.

1 Introduction

Schulz [1] presented an integrated beam formulation where an arbitrary cross-section remains neither plane nor orthogonal to the beam axis.

This theory is based on the finite-element formulation proposed by Kazic and Dong [2] for linear-elastic and arbitrary cross-sections, which is based on the minimization of the potential energy of an infinitesimal beam slice. Semi-analytical methods were studied by Dong, Kosmatka and Lin [3] and Lin and Dong [4], for Saint-Venant's [5] and Michell's [6] problems, respectively.

The kinematics of the proposed beam element is defined by two fields: the displacement shapes of the cross-sections and the axial functions of their corresponding averaged movements. The energy methodology proposed in Kazic and Dong [3] is augmented with constraints that ensure compatibility between the displacement fields. This approach establishes a recursive procedure that yields higher order deformed displacement shapes, which is initiated with the rigid-body components of the displacement field. Higher order models reproduce the three-dimensional distribution of stresses and strains of Elasticity solutions and correspond well with three-dimensional linear and nonlinear finite element models, with idealized boundary conditions. The formulation is limited to small displacements and the constitutive matrix is considered always positive-definite.

This paper presents improvements that simplify the theory and focuses on first-order linear and nonlinear analyses. Examples of linear and nonlinear analyses are presented.

2 Beam element kinematics

A beam with an arbitrary cross-section is shown in Figure 1. The current investigation considers that the displacements are small, and the constitutive matrix is positive-definite. The material and geometrical characteristics are constant along the axis of the beam. Disturbed states of deformation at the boundaries are not considered.

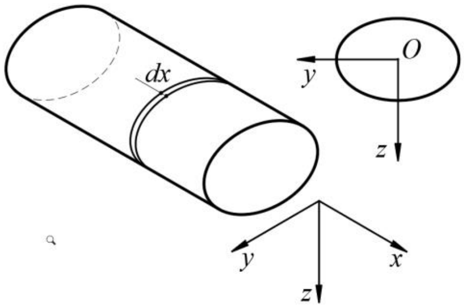

Figure 1. Beam coordinates

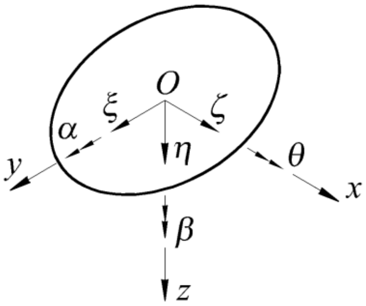

Figure 2. Displacements and rotations of the cross section

The displacement vector $\mathbf{u} = \begin{bmatrix} u_x & u_y & u_z \end{bmatrix}^T$ is arranged as follows:

$$\mathbf{u}_x = \begin{bmatrix} u_x & 0 & 0 & u_y & 0 & u_z \end{bmatrix}^T \quad ; \quad \mathbf{u}_y = \begin{bmatrix} 0 & u_y & 0 & u_x & u_z & 0 \end{bmatrix}^T \quad ; \quad \mathbf{u}_z = \begin{bmatrix} 0 & 0 & u_z & 0 & u_y & u_x \end{bmatrix}^T \tag{1}$$

The strain vector $\boldsymbol{\varepsilon} = \begin{bmatrix} \varepsilon_x & \varepsilon_y & \varepsilon_z & \gamma_{xy} & \gamma_{yz} & \gamma_{zx} \end{bmatrix}^T$ is expressed by

$$\boldsymbol{\varepsilon} = \mathbf{u}_{x,x} + \mathbf{u}_{y,y} + \mathbf{u}_{z,z} \tag{2}$$

where $f_{i,j} = \partial f_i / \partial x_j$.

The stress vector $\boldsymbol{\sigma} = \begin{bmatrix} \sigma_x & \sigma_y & \sigma_z & \tau_{xy} & \tau_{yz} & \tau_{zx} \end{bmatrix}^T$ is arranged as follows:

$$\boldsymbol{\sigma}_x = \begin{bmatrix} \sigma_x & \tau_{xy} & \tau_{zx} \end{bmatrix}^T \quad ; \quad \boldsymbol{\sigma}_y = \begin{bmatrix} \tau_{xy} & \sigma_y & \tau_{yz} \end{bmatrix}^T \quad ; \quad \boldsymbol{\sigma}_z = \begin{bmatrix} \tau_{zx} & \tau_{yz} & \sigma_z \end{bmatrix}^T \tag{3}$$

Distributed loads are considered in Schulz[1], but they are not discussed in this paper for simplicity. The equilibrium equations are expressed as

$$\boldsymbol{\sigma}_{x,x} + \boldsymbol{\sigma}_{y,y} + \boldsymbol{\sigma}_{z,z} = \mathbf{0} \tag{4}$$

The cross-section is discretized by the finite element method. Displacements and their derivatives are interpolated by

$$\mathbf{u} = \mathbf{N}\mathbf{U} \quad ; \quad \mathbf{u}_x = \mathbf{N}_x \mathbf{U} \quad ; \quad \mathbf{u}_y = \mathbf{N}_y \mathbf{U} \quad ; \quad \mathbf{u}_z = \mathbf{N}_z \mathbf{U} \tag{5}$$

$$\mathbf{u}_{x,x} = \mathbf{N}_x \mathbf{U}' \quad ; \quad \mathbf{u}_{y,y} = \mathbf{N}_{y,y} \mathbf{U} \quad ; \quad \mathbf{u}_{z,z} = \mathbf{N}_{z,z} \mathbf{U} \tag{6}$$

$\mathbf{U}$ is of the nodal displacement vector of the cross-section and $f' = f_{,x}$. $\mathbf{N}$, $\mathbf{N}_i$, and $\mathbf{N}_{i,j}$ are interpolation matrices. The compatibility equation (2) is rewritten as

$$\boldsymbol{\varepsilon} = \mathbf{N}_A \mathbf{U} + \mathbf{N}_L \mathbf{U}' \tag{7}$$

where $\mathbf{N}_A = \mathbf{N}_{y,y} + \mathbf{N}_{z,z}$ and $\mathbf{N}_L = \mathbf{N}_x$.

The constitutive relation for nonlinear hyperplastic materials is expressed by

$$\boldsymbol{\sigma} = \boldsymbol{\sigma}(\boldsymbol{\varepsilon}) \quad ; \quad \Delta\boldsymbol{\sigma} = \mathbf{C}(\boldsymbol{\varepsilon})\, \Delta\boldsymbol{\varepsilon} \tag{8}$$

Equation (8) yields $\boldsymbol{\sigma} = \mathbf{C}\boldsymbol{\varepsilon}$ for isotropic and orthotropic linear elastic materials.

The rigid-body movements of the cross-section are expressed by the displacements ζ , ξ and η in the *x*-, *y*-

and z-directions, respectively, and rotations θ, α and β about the x-, y- and z-axes, respectively (Figure 2). A rigid-body movement $\bar{\mathbf{U}}$ of the cross-section is represented by

$$\bar{\mathbf{U}} = \bar{\mathbf{M}}\mathbf{\Phi} \tag{9}$$

where $\bar{\mathbf{M}} = \left[\bar{\mathbf{U}}_\zeta \ \vdots\ \bar{\mathbf{U}}_\xi \ \vdots\ \bar{\mathbf{U}}_\eta \ \vdots\ \bar{\mathbf{U}}_\theta \ \vdots\ \bar{\mathbf{U}}_\alpha \ \vdots\ \bar{\mathbf{U}}_\beta\right]$ is the rigid-body displacement matrix of the cross-section and $\mathbf{\Phi} = \left[\zeta \quad \xi \quad \eta \quad \theta \quad \alpha \quad \beta\right]^T$.

The averaged 3D movement $\mathbf{\Phi}$ of a displacement shape $\mathbf{U}$ is defined as a movement that minimizes a functional $f_{\mathrm{U}} = \int_A \left(\mathbf{U}-\bar{\mathbf{U}}\right)^T \mathbf{W}\left(\mathbf{U}-\bar{\mathbf{U}}\right) dA$, where $\mathbf{W} = \mathbf{N}_L^T\mathbf{C}\mathbf{N}_L$. This definition yields

$$\mathbf{\Phi} = \mathbf{\Omega}^T\mathbf{U} \quad ; \quad \phi = \mathbf{\Omega}_\phi^T\mathbf{U} \tag{10}$$

where $\phi = \zeta,\ \xi,\ \eta,\ \theta,\ \alpha$ and β and $\mathbf{\Omega}_\phi$ is the ϕ^{th} column of $\mathbf{\Omega}$. The weighting matrix $\mathbf{\Omega}$ is established by

$$\mathbf{\Omega} = \mathbf{K}_{LL}\bar{\mathbf{M}}^* \quad ; \quad \mathbf{\Omega}_\phi = \mathbf{K}_{LL}\bar{\mathbf{U}}_\phi^* \tag{11}$$

$$\mathbf{K}_{LL} = \int_A \mathbf{N}_L^T\,\mathbf{C}\,\mathbf{N}_L\,dA \quad ; \quad \bar{\mathbf{M}}^* = \bar{\mathbf{M}}\left(\bar{\mathbf{M}}^T\mathbf{K}_{LL}\bar{\mathbf{M}}\right)^{-1} \tag{12}$$

The pre-multiplication of both sides of (11) by $\bar{\mathbf{M}}^T$ yields

$$\bar{\mathbf{M}}^T\mathbf{\Omega} = \mathbf{\Omega}^T\bar{\mathbf{M}} = \mathbf{I} \tag{13}$$

3 Equilibrium equation

An infinitesimal beam slice is defined as the volume of the beam which length is an infinitesimal distance dx (Figure 3). The variation of the potential energy is expressed as

$$\delta\Pi = \int_A \delta\boldsymbol{\varepsilon}^T\boldsymbol{\sigma}\,dA - \int_A \delta\mathbf{u}_{,x}^T\,\boldsymbol{\sigma}_x\,dA - \int_A \delta\mathbf{u}^T\boldsymbol{\sigma}_{x,x}\,dA \tag{14}$$

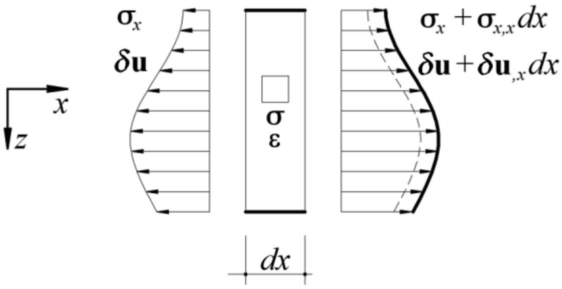

Figure 3. Infinitesimal beam slice

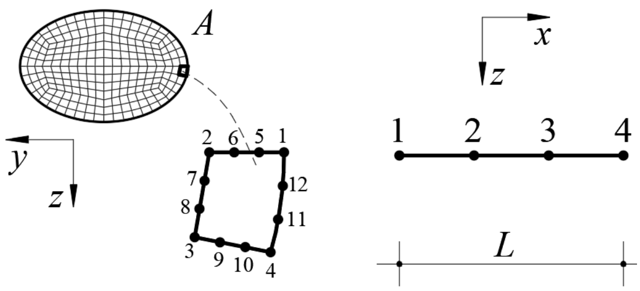

Figure 4. Cross-section and beam finite elements

The substitution of (2) in (14) yields

$$\delta\Pi = \int_A \left(\delta\mathbf{u}_{y,y}^T + \delta\mathbf{u}_{z,z}^T\right)\boldsymbol{\sigma}\,dA - \int_A \delta\mathbf{u}_x^T\,\boldsymbol{\sigma}_{,x}\,dA \tag{15}$$

The averaged movements of the cross-sections must satisfy a beam kinematic framework. The constraint functions g_ϕ are defined as $g_\phi\left(\mathbf{U}\right) = \mathbf{U}^T\mathbf{\Omega}_\phi - \phi_x = 0$. With (6), the substitution of (15) in the stationary condition of a Lagrangian function expressed by $\Lambda\left(\mathbf{U}\right) = \Pi\left(\mathbf{U}\right) + \sum \lambda_\phi g_\phi\left(\mathbf{U}\right)$, leads to the equilibrium equation

$$\int_A \mathbf{N}_A^T\boldsymbol{\sigma}\,dA = \int_A \mathbf{N}_L^T\,\boldsymbol{\sigma}_{,x}\,dA + \mathbf{\Omega}\boldsymbol{\lambda} \tag{16}$$

where $\boldsymbol{\lambda} = \left[\lambda_\zeta \quad \lambda_\xi \quad \lambda_\eta \quad \lambda_\theta \quad \lambda_\alpha \quad \lambda_\beta\right]^T$ are the Lagrange multipliers being added to the original formulation proposed by Kazic and Dong [2]. Equation (16) is valid for linear and nonlinear materials.

4 Linear elastic materials

Linear elastic beams with constant material and geometrical characteristics yield $\boldsymbol{\sigma} = \mathbf{C}\boldsymbol{\varepsilon}$ and $\mathbf{C}' = \mathbf{0}$. The substitution of (5) and (6) into (16) results in

$$\mathbf{K}_{AA}\,\mathbf{U} = \left[\mathbf{K}_{LA} - \mathbf{K}_{AL}\right]\mathbf{U}' + \mathbf{K}_{LL}\,\mathbf{U}'' + \boldsymbol{\Omega}\boldsymbol{\lambda} \tag{17}$$

$$\mathbf{K}_{AA} = \int_A \mathbf{N}_A^T \mathbf{C}\mathbf{N}_A\, dA \quad ; \quad \mathbf{K}_{LA} = \mathbf{K}_{AL}^T = \int_A \mathbf{N}_L^T \mathbf{C}\mathbf{N}_A\, dA \tag{18}$$

Higher-order formulations are presented in Schulz [1]. The discussion here is limited to first-order formulations, for simplicity. The displacement field $\mathbf{U}$ of the first-order formulation is defined as

$$\begin{aligned}
\mathbf{U} &= \zeta\bar{\mathbf{U}}_\zeta + \xi\bar{\mathbf{U}}_\xi + \eta\bar{\mathbf{U}}_\eta + \theta\bar{\mathbf{U}}_\theta + \alpha\bar{\mathbf{U}}_\alpha + \beta\bar{\mathbf{U}}_\beta + \\
&\quad + \zeta'\tilde{\mathbf{U}}_\zeta^1 + \left(\xi' - \beta\right)\tilde{\mathbf{U}}_\xi^1 + \left(\eta' + \alpha\right)\tilde{\mathbf{U}}_\eta^1 + \theta'\tilde{\mathbf{U}}_\theta^1 + \alpha'\tilde{\mathbf{U}}_\alpha^1 + \beta'\tilde{\mathbf{U}}_\beta^1 \\
\mathbf{U}' &= \zeta'\bar{\mathbf{U}}_\zeta + \xi'\bar{\mathbf{U}}_\xi + \eta'\bar{\mathbf{U}}_\eta + \theta'\bar{\mathbf{U}}_\theta + \alpha'\bar{\mathbf{U}}_\alpha + \beta'\bar{\mathbf{U}}_\beta = -\alpha\bar{\mathbf{U}}_\eta + \beta\bar{\mathbf{U}}_\xi + \\
&\quad + \zeta'\bar{\mathbf{U}}_\zeta + \left(\xi' - \beta\right)\bar{\mathbf{U}}_\xi + \left(\eta' + \alpha\right)\bar{\mathbf{U}}_\eta + \theta'\bar{\mathbf{U}}_\theta + \alpha'\bar{\mathbf{U}}_\alpha + \beta'\bar{\mathbf{U}}_\beta \\
\mathbf{U}'' &= -\alpha'\bar{\mathbf{U}}_\eta + \beta'\bar{\mathbf{U}}_\xi
\end{aligned} \tag{19}$$

Terms $\left(\xi' - \beta\right)$ and $\left(\eta' + \alpha\right)$ are the shear distortions of the cross-sections. $\tilde{\mathbf{U}}_\phi^1$ are the first deformed shapes of $\phi = \zeta,\ \xi,\ \eta,\ \theta,\ \alpha$ and β. In a first-order formulation, the polynomial expansions are truncated at

$$\zeta'' = \left(\xi' - \beta\right)' = \left(\eta' + \alpha\right)' = \theta'' = \alpha'' = \beta'' = 0 \tag{20}$$

but $\alpha' \neq 0$ and $\beta' \neq 0$. The following properties apply:

$$\mathbf{N}_A\bar{\mathbf{U}}_\phi = \begin{bmatrix}0 & 0 & 0 & 0 & 0 & 0\end{bmatrix}^T \quad \text{for } \phi = \zeta,\ \xi,\ \eta \text{ and } \theta \tag{21}$$

$$\mathbf{N}_L\bar{\mathbf{U}}_\xi = -\mathbf{N}_A\bar{\mathbf{U}}_\beta = \begin{bmatrix}0 & 0 & 0 & 1 & 0 & 0\end{bmatrix}^T \tag{22}$$

$$\mathbf{N}_L\bar{\mathbf{U}}_\eta = \mathbf{N}_A\bar{\mathbf{U}}_\alpha = \begin{bmatrix}0 & 0 & 0 & 0 & 0 & 1\end{bmatrix}^T \tag{23}$$

$$\mathbf{K}_{AA}\bar{\mathbf{U}}_\phi = \mathbf{0} \quad \text{for } \phi = \zeta,\ \xi, \eta \text{ and } \theta \tag{24}$$

$$\mathbf{K}_{LA}\bar{\mathbf{U}}_\phi = \mathbf{0} \quad \text{for } \phi = \zeta,\ \xi, \eta \text{ and } \theta \tag{25}$$

$$\mathbf{K}_{AA}\bar{\mathbf{U}}_\beta = -\mathbf{K}_{AL}\bar{\mathbf{U}}_\xi \quad ; \quad \mathbf{K}_{AA}\bar{\mathbf{U}}_\alpha = \mathbf{K}_{AL}\bar{\mathbf{U}}_\eta \tag{26}$$

$$\mathbf{K}_{LA}\bar{\mathbf{U}}_\beta = -\mathbf{K}_{LL}\bar{\mathbf{U}}_\xi \quad ; \quad \mathbf{K}_{LA}\bar{\mathbf{U}}_\alpha = \mathbf{K}_{LL}\bar{\mathbf{U}}_\eta \tag{27}$$

The substitution of (19) and (21) to (27) into (17) yields

$$\mathbf{K}_{AA}\tilde{\mathbf{U}}_\phi^1 = -\mathbf{K}_{AL}\bar{\mathbf{U}}_\phi + \boldsymbol{\Omega}\lambda_\phi \quad \text{for } \phi = \zeta,\ \xi,\ \eta,\ \theta,\ \alpha, \text{ and } \beta \tag{28}$$

where $\boldsymbol{\lambda}_\phi = \begin{bmatrix}\lambda_{\phi\zeta} & \lambda_{\phi\xi} & \lambda_{\phi\eta} & \lambda_{\phi\theta} & \lambda_{\phi\alpha} & \lambda_{\phi\beta}\end{bmatrix}^T$.

Stiffness matrix $\mathbf{K}_{AA}$ is symmetric but, as indicated in (24), rigid body displacements $\bar{\mathbf{U}}_\phi$ must be isostatically restrained for $\phi = \zeta,\ \xi,\ \eta$ and θ. Equation (28) is rewritten as

$$\tilde{\mathbf{U}}_\phi^1 = -\mathbf{K}_{AA}^{-1}\mathbf{K}_{AL}\bar{\mathbf{U}}_\phi + \mathbf{K}_{AA}^{-1}\boldsymbol{\Omega}\lambda_\phi \quad \text{for } \phi = \zeta,\ \xi,\ \eta,\ \theta,\ \alpha, \text{ and } \beta \tag{29}$$

The averaged displacements of the deformed shapes must be zero, i.e.

$$\boldsymbol{\Phi}_\phi = \boldsymbol{\Omega}^T\tilde{\mathbf{U}}_\phi^1 = \mathbf{0} \tag{30}$$

Pre-multiplying both sides of (29) by $\boldsymbol{\Omega}^T$ and substituting (30) yield

$$\left(\boldsymbol{\Omega}^T\mathbf{K}_{AA}^{-1}\boldsymbol{\Omega}\right)\lambda_\phi = \boldsymbol{\Omega}^T\mathbf{K}_{AA}^{-1}\mathbf{K}_{AL}\bar{\mathbf{U}}_\phi \tag{31}$$

The Lagrange multipliers λ_ϕ are obtained by solving the system of equations (31). Equation (29) yields the first-order deformed shapes $\tilde{\mathbf{U}}_\phi^1$.

The substitution of (19) to (23) in (7) yields the following expressions for first-order formulation strains:

$$\boldsymbol{\varepsilon}' \simeq \mathbf{0} \tag{32}$$

$$\boldsymbol{\varepsilon} = \mathbf{E}\,\mathbf{e} \tag{33}$$

where

$$\mathbf{E} = \begin{bmatrix} \mathbf{E}_{\zeta'} & \mathbf{E}_{\xi'} & \mathbf{E}_{\eta'} & \mathbf{E}_{\theta'} & \mathbf{E}_{\alpha'} & \mathbf{E}_{\beta'} \end{bmatrix} \quad ; \quad \mathbf{E}_{\phi'} = \mathbf{N}_A \tilde{\mathbf{U}}_\phi + \mathbf{N}_L \bar{\mathbf{U}}_\phi \tag{34}$$

$$\mathbf{e} = \begin{bmatrix} \zeta' & (\xi' - \beta) & (\eta' + \alpha) & \theta' & \alpha' & \beta' \end{bmatrix}^T \tag{35}$$

Strain equation (33) and standard procedures of the finite element method yield the beam element stiffness matrix of the first-order formulation.

5 Hyperelastic nonlinear materials

For hyperelastic nonlinear materials, the substitution of (8) in (16) leads to

$$\int_A \mathbf{N}_A^T \boldsymbol{\sigma}\, dA = \int_A \mathbf{N}_L^T \mathbf{C}\boldsymbol{\varepsilon}'\, dA + \boldsymbol{\Omega\lambda} \tag{36}$$

Considering (32), (36) simplifies to the following nonlinear equilibrium equation:

$$\mathbf{r} = \int_A \mathbf{N}_A^T \boldsymbol{\sigma}\, dA - \boldsymbol{\Omega\lambda} = \mathbf{0} \tag{37}$$

Equation (33) can be rewritten as

$$\boldsymbol{\varepsilon} = \mathbf{N}_A \tilde{\mathbf{U}} + \bar{\mathbf{E}}\,\mathbf{e} \tag{38}$$

where $\tilde{\mathbf{U}}$ denotes a deformed displacement vector of the cross-section and

$$\bar{\mathbf{E}} = \begin{bmatrix} \bar{\mathbf{E}}_{\zeta'} & \bar{\mathbf{E}}_{\xi'} & \bar{\mathbf{E}}_{\eta'} & \bar{\mathbf{E}}_{\theta'} & \bar{\mathbf{E}}_{\alpha'} & \bar{\mathbf{E}}_{\beta'} \end{bmatrix} \quad ; \quad \bar{\mathbf{E}}_{\phi'} = \mathbf{N}_L \bar{\mathbf{U}}_\phi \tag{39}$$

Each iterative step of the model analysis starts with a previous approximation of the nodal displacements $\mathbf{U}_B$ of the beam.

At each integration point, the interpolation $\mathbf{e} = \mathbf{B}\ \mathbf{U}_B$ establishes the strains associated with the rigid-body movements of the beam. However, deformed displacement $\tilde{\mathbf{U}}$ are unknown. An iterative procedure is therefore necessary, for each integration point, and it starts with the previous approximation of $\tilde{\mathbf{U}}$. Equilibrium is achieved when $\Delta\mathbf{r} = \mathbf{0} - \mathbf{r} \simeq 0$. Expressions (8) and (37) yield the following linearized incremental equation:

$$\int_A \mathbf{N}_A^T \mathbf{C}\, \Delta\boldsymbol{\varepsilon}\, dA = \Delta\mathbf{r} + \boldsymbol{\Omega}\, \Delta\boldsymbol{\lambda} \tag{40}$$

Considering that strains $\mathbf{e}$ associated with rigid-body movements are known, equation (38) yields

$$\Delta\boldsymbol{\varepsilon} = \mathbf{N}_A\, \Delta\tilde{\mathbf{U}} \tag{41}$$

The substitution of (18) and (41) in (40) yields

$$\mathbf{K}_{AA}\, \Delta\tilde{\mathbf{U}} = \Delta\mathbf{r} + \boldsymbol{\Omega}\, \Delta\boldsymbol{\lambda} \tag{42}$$

Stiffness matrix $\mathbf{K}_{AA}$ is symmetric but, as indicated in (24), rigid body displacements $\bar{\mathbf{U}}_\phi$ must be isostatically restrained for $\phi = \zeta,\ \xi,\ \eta$ and θ. Equation (42) is rewritten as

$$\Delta\tilde{\mathbf{U}} = \mathbf{K}_{AA}^{-1}\, \Delta\mathbf{r} + \mathbf{K}_{AA}^{-1}\, \boldsymbol{\Omega}\, \Delta\boldsymbol{\lambda} \tag{43}$$

The averaged displacement of the deformed displacements $\Delta\tilde{\mathbf{U}}$ must be zero, i.e.

$$\boldsymbol{\Phi} = \boldsymbol{\Omega}^T \Delta\tilde{\mathbf{U}} = \mathbf{0} \tag{44}$$

Pre-multiplying both sides of (43) by $\boldsymbol{\Omega}^T$ and substituting (44) yield

$$\left(\boldsymbol{\Omega}^T \mathbf{K}_{AA}^{-1} \boldsymbol{\Omega}\right)\Delta\boldsymbol{\lambda} = -\boldsymbol{\Omega}^T \mathbf{K}_{AA}^{-1} \Delta\mathbf{r} \tag{45}$$

The Lagrange multipliers $\Delta\boldsymbol{\lambda}$ are obtained by solving of the system of equations defined in (45). Equation (43) yields the incremental deformed strains $\Delta\tilde{\mathbf{U}}$.

An iterative process at each integration point leads to the corresponding deformed displacement $\tilde{\mathbf{U}}$. Strains are evaluated with (38) and standard procedures of the finite element method yield the tangent stiffness matrix of the beam element.

6 Implementation

The cross-section is discretized by 12-node isoparametric finite-elements and three degrees of freedom per node (Figure 4).

The beam elements are defined with four nodes and six degrees of freedom per node (Figure 4).

The location of the beam's $x-$axis is independent of the mesh discretization of the cross section.

7 Examples

7.1 Example 1

The first example is a linear elastic cantilever beam with a tip load and elliptical cross-section (Figure 5). The first-order approach yields a tip deflection $u_z = 0.144543 \times 10^{-03}$ when using a single or 20 beam elements.

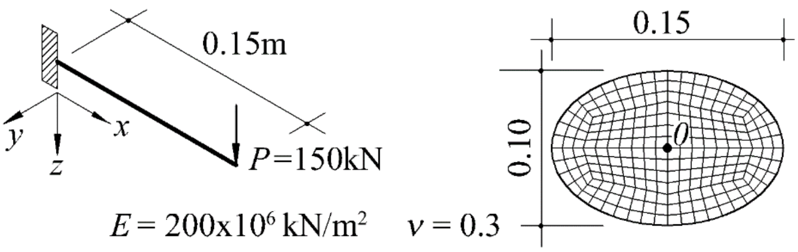

Figure 5. Example 1: Linear elastic beam with elliptical cross-section

Figure 6 shows the normal and shear stresses of a cross section at the support.

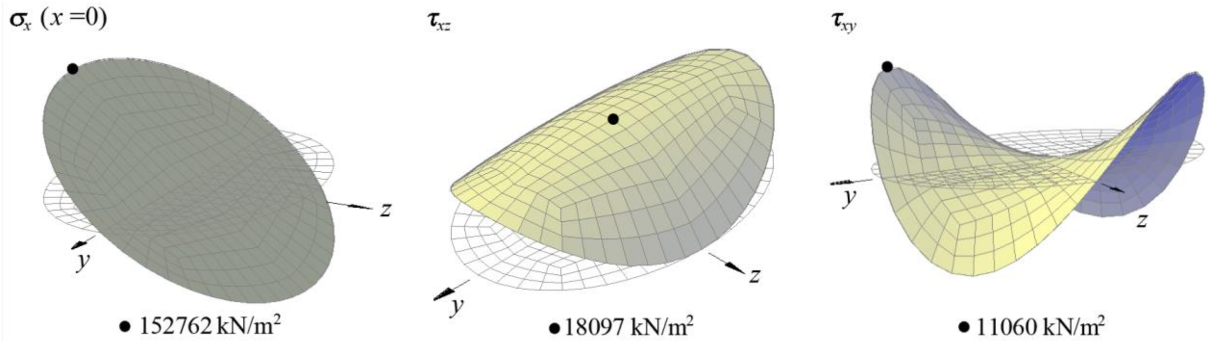

Figure 6. Example 1: Normal and shear stresses at x = 0 m

7.2 Example 2

The second example a cantilever beam made of an hyperelastic material (Figure 7). The beam has a hexagonal cross-section and is subjected to a tip load. This study is carried out with 20 beam elements.

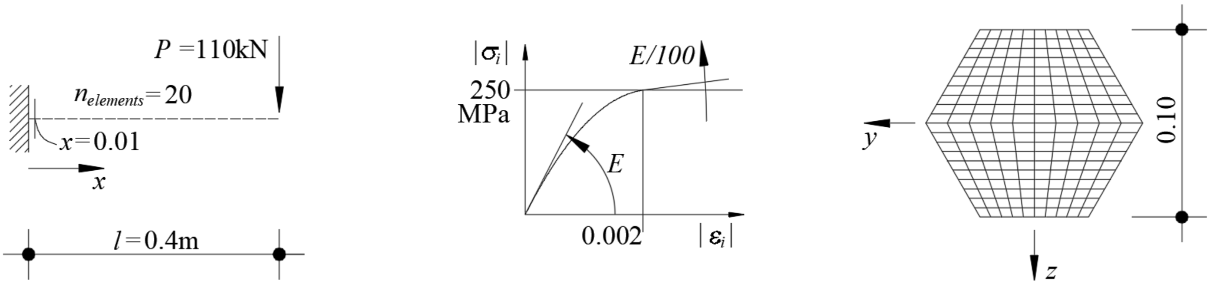

Figure 7. Example 2: Hyperelastic beam with hexagonal cross-section

Figure 6 shows the normal and shear stresses of a cross section near the support. The shear stresses are approximately zero at the ends where normal stresses reach the yield point.

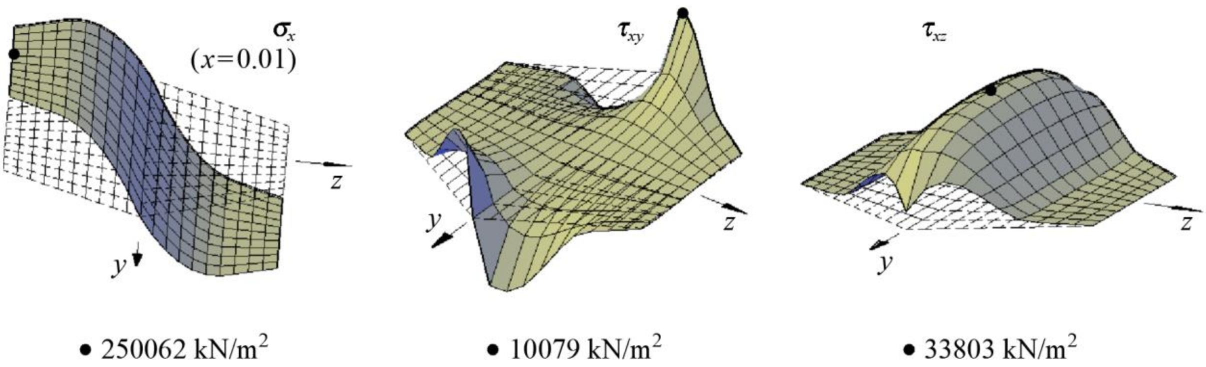

Figure 8. Example 2: Normal and shear stresses at x = 0.01 m

8 Conclusion

3D-response beams are easily introduced in standard finite element programs. All formulations are free from shear coefficients. The linear elastic formulation is very efficient because the stiffness matrix of the cross-section is inverted only once. The proposed beam elements can use 3D nonlinear stress-strain relationships.

Authorship statement. The authors hereby confirm that they are the sole liable persons responsible for the authorship of this work, and that all material that has been herein included as part of the present paper is either the property (and authorship) of the authors or has the permission of the owners to be included here.

References

[1] M. Schulz, “Beam Element with a 3D Response for Shear Effects”. *Journal of Engineering Mechanics*, ASCE, v.144(1): 04017149, 2018.

[2] M. Kazic and S. B. Dong (1990). "Analysis of restrained torsion." *J. Eng. Mech.* - ASCE, 116(4), 870-891.

[3] S. B. Dong, J. B. Kosmatka, and H. C. Lin (2001). "On Saint-Venant’s problem for an inhomogeneous, anisotropic cylinder - part I: methodology for Saint-Venant solutions." J. Appl. Mech. - ASME, 68(3), 376-381.

[4] H. C. Lin and S. B. Dong (2006). "On the Almansi-Michell problems for an inhomogeneous, anisotropic cylinder." *J. Mech.*, 22(01), 51-57.

[5] Saint-Venant, A. J. C. B. (1856). "Mémoire sur la flexion des prismes." *J. Math. Pure Appl.*, s.2(v.1), 89-189.

[6] Michell, J. H. (1901). "The theory of uniformly loaded beams." *Quart. J. Pure Appl. Math.*, 32, 28-42.